Biochimica et Biophysica Acta 1838 (2014) 2767–2777

Contents lists available at ScienceDirect

Biochimica et Biophysica Acta

journal homepage: www.elsevier.com/locate/bbamem

Guanylate Cyclase-Activating Protein-2 Undergoes Structural Changes upon Binding to Detergent Micelles and Bicelles

Aleksandra Margetić [a,b], David Nannemann [c], Jens Meiler [c], Daniel Huster [b,d,*], Stephan Theisgen [b]

[a] Institute of Chemistry, Technology and Metallurgy, Center of Chemistry, University of Belgrade, Studentski trg 12-16, 11000 Belgrade, Serbia
[b] Institute of Medical Physics and Biophysics, University of Leipzig, Härtelstr. 16-18, D-04107 Leipzig, Germany
[c] Center for Structural Biology, Vanderbilt University, 465 21st Ave South, Nashville, TN, USA
[d] Department of Chemical Sciences, Tata Institute of Fundamental Research, Homi Bhabha Road, Colaba, Mumbai 400 005, India

ARTICLE INFO

Article history:
Received 11 June 2014
Received in revised form 11 July 2014
Accepted 14 July 2014
Available online 19 July 2014

Keywords:
GCAP-2
membrane-protein interaction
myristoyl switch
bicelles
solution NMR
ROSETTA

ABSTRACT

GCAPs are neuronal Ca^{2+}-sensors playing a central role in light adaptation. GCAPs are N-terminally myristoylated membrane-associated proteins. Although, the myristoylation of GCAPs plays an important role in light adaptation its structural and physiological roles are not yet clearly understood. The crystal-structure of GCAP-1 shows the myristoyl moiety inside the hydrophobic core of the protein, stabilizing the protein structure; but ^{2}H-solid-state NMR investigations on the deuterated myristoyl moiety of GCAP-2 in the presence of liposomes showed that it is inserted into the lipid bilayer. In this study, we address the question of the localization of the myristoyl group of Ca^{2+}-bound GCAP-2, and the influence of CHAPS-, DPC-micelles and DMPC/DHPC-bicelles on the structure, and on the localization of the myristoyl group, of GCAP-2 by solution-state NMR. We also carried out the backbone assignment. Characteristic chemical shift differences have been observed between the myristoylated and the non-myristoylated forms of the protein. Our results support the view that in the absence of membrane forming substances the myristoyl moiety is buried inside a hydrophobic pocket of GCAP-2 similar to the crystal structure of GCAP-1. Addition of CHAPS-micelles and DMPC/DHPC-bicelles cause specific structural changes localized in and around the myristoyl binding pocket. We interpret these changes as an indication for the extrusion of the myristoyl moiety from its binding pocket and its insertion into the hydrophobic interior of the membrane mimic. On the basis of the backbone chemical shifts, we propose a structural model of myristoylated GCAP-2 in the presence of Ca^{2+} and membrane mimetics.

1. Introduction

Guanylate cyclase-activating proteins (GCAPs) are neuronal Ca^{2+}-sensors playing a central role in light adaptation through the Ca^{2+}-dependent regulation of the retinal guanylate cyclase. They belong to the superfamily of calmodulin-like four EF hand Ca^{2+} binding proteins, whereas the first EF hand is not able to bind Ca^{2+} [1,2].

GCAPs are N-terminally myristoylated, membrane-associated proteins [3]. Although, the myristoylation of GCAP plays an important role in light adaptation [4–6] its structural and physiological roles are not yet clearly understood. The myristoyl moiety can in principle be buried inside the hydrophobic core or in a hydrophobic pocket of the protein, where it may exert a structure-stabilizing function as shown for the poliovirus VP4 protein [7] and the protein kinase A [8]. But more frequently, lipid modifications serve as membrane anchors and are consequently exposed to the surrounding medium [9–11] at least upon membrane binding.

A switch mechanism from a protein embedded to a solvent exposed or membrane inserted myristoyl chain has been shown for the closely related proteins recoverin [12], neurocalcin δ [13], and hippocalcin [14]. In these examples, the lipid modified soluble proteins are found in two states. State I represents the soluble form, where the lipid modification is buried within the hydrophobic interior, and state II is the membrane bound form, in which the lipid chain is released from the protein interior and inserted into the lipid membrane. Such a mechanism is best described for recoverin, where highly resolved structures of both states have been solved by solution NMR spectroscopy [15]. For recoverin, the two states are controlled by the intracellular Ca^{2+}

Abbreviations: CHAPS, 3-[(3-Cholamidopropyl)dimethylammonio]-1-propanesulfonate; DHPC, 1,2-diheptanoyl-*sn*-glycero-3-phosphocholine; DMPC, 1,2-dimyristoyl-*sn*-glycero-3-phosphocholine; DPC, dodecylphosphocholine; DTT, DL-dithiothreitol; EDTA, ethylenediaminetetraacetic acid; FCaBP, flagellar calcium-binding protein; GCAP, guanylate cyclase-activating protein; HSQC, hetero single quantum coherence; IPTG, isopropyl-β-D-1-thiogalactopyranoside; MALDI-TOF, matrix-assisted laser desorption/ionization time-of-flight mass spectrometry; MWCO, molecular weight cut-off; NCS-1, neuronal calcium sensor-1; NMR, nuclear magnetic resonance spectroscopy; NS, number of scans; PDB, protein data bank (www.pdb.org); RP-HPLC, reversed-phase high-performance liquid chromatography; SDS-PAGE, sodium dodecyl sulfate polyacrylamide gel electrophoresis; TCEP, tris(2-carboxyethyl)phosphine; TFA, trifluoroacetic acid; Tris, 2-amino-2-hydroxymethyl-propane-1,3-diol

* Corresponding author at: Institute of Medical Physics and Biophysics, Härtelstr. 16-18, D-04107 Leipzig. Tel.: +49 341 97 15701; fax: +49 341 97 15709.
E-mail address: daniel.huster@medizin.uni-leipzig.de (D. Huster).

http://dx.doi.org/10.1016/j.bbamem.2014.07.012
0005-2736/

levels. This structural change upon Ca^{2+} binding is called the Ca^{2+}-myristoyl switch mechanism. The Ca^{2+}-free form of recoverin has the myristoyl moiety buried inside the hydrophobic core, but Ca^{2+}-binding leads to the exposure of the myristoyl moiety and hence to the membrane binding of the protein [12,15–18].

Additionally, in the case of GCAPs, the myristoyl moiety could also function as an activator for the guanylate cyclase through an interaction with a dedicated binding site. In agreement with this assumption, myristoylated GCAPs are better activators than the non-myristoylated ones and myristoylated GCAP-1 has a sevenfold higher affinity for the guanylate cyclase than non-myristoylated GCAP-1 [4].

Currently, only the structures of Ca^{2+}-bound, non-myristoylated GCAP-2, solved by solution-state NMR spectroscopy [19], Ca^{2+}-bound, myristoylated GCAP-1 [20] and Ca^{2+}-bound, non-myristoylated GCAP-3 [21] solved by X-ray crystallography, are available. The crystal structure of myristoylated GCAP-1 shows the myristic acid inside the hydrophobic core of the protein; therefore, the authors postulated a structure-stabilizing function of the myristic acid [20]. In contrast, Vogel et al. performed ^{2}H solid-state NMR investigations on the deuterated myristoyl moiety of Ca^{2+}-free GCAP-2 in the presence of liposomes and demonstrated that the myristoyl moiety is inserted into the lipid bilayer of the membrane [22].

Both studies provide some insights with regard to the localization and the functional role of the myristoyl moiety of GCAP-2, even if they appear contradictory at first sight. However, there are relevant differences in these studies: first, the crystal structure shows GCAP-1 [20] but Vogel et al. investigated GCAP-2 [22]. Despite the close relationship and relatively high homology, the role of the myristoyl moiety could be different for both isoforms. Second, the environment in a protein crystal differs significantly from that in solution and is again very different from the conditions at the membrane surface. It is possible that the tight packing in the crystal forces the myristic acid inside the protein as a requirement for the crystallization to occur. As a free lipid chain acquires high mobility to reduce the free energy through an increase in the configurational entropy [9,23,24], highly mobile (side) chains typically represent a barrier for crystallization. Furthermore, the crystal structure represents the Ca^{2+}-bound state, whereas Vogel et al. investigated the Ca^{2+}-free form [22]. Therefore, it could be possible, that an 'inverse' Ca^{2+}-myristoyl switch mechanism (opposite to that of recoverin) is present, such that in the Ca^{2+}-bound state the myristic acid is buried inside the hydrophobic core of the protein, but in the Ca^{2+}-free state the myristoyl moiety is released and inserted into the membrane. Most reports interpret their data against a Ca^{2+}-myristoyl-switch, but some claim that they cannot exclude it [5,6,25,26]. In biophysical studies, we confirmed, that the myristic moiety is indeed inserted into the membrane in the Ca^{2+}-free as well as in the Ca^{2+}-bound state [27], again finding no evidence for an inverse myristoyl switch. Based on these data, however, we proposed a different model, according to which soluble GCAP-2 protein features the myristoyl moiety sequestered inside a hydrophobic binding site of the protein, upon membrane binding the high local concentration of lipids favors and triggers the insertion of the myristoyl moiety into the lipid bilayer.

In this study, we first address the question of the localization of the myristoyl group of GCAP-2 in solution. Then, we study if a membrane-like environment induces structural alterations of the protein that would suggest a translocation of the myristoyl moiety from the protein interior into the hydrophobic interior of a membrane. To address these question by solution NMR, we studied structural alterations of GCAP-2 in the presence of the non-denaturing micelle-forming detergent CHAPS, the detergent DPC, carrying the same head group as the main phospholipids, and DMPC/DHPC bicelles as the most membrane-like structures amenable to solution-state NMR. As a prerequisite for this analysis, we carried out the NMR assignment of the backbone of myristoylated GCAP-2 and determined a structural model of the protein using CS-ROSETTA [28].

2. Material and Methods

2.1. Materials

Dodecylphosphocholine-d_{38}, $^{15}NH_4Cl$ and D-glucose (U-^{13}C, 99%) were purchased from Cambridge Isotope Laboratories (Andover, USA). 1,2-Diheptanoyl-*sn*-glycero-3-phosphocholine (DHPC) and 1,2-dimyristoyl-*sn*-glycero-3-phosphocholine (DMPC) were purchased from Avanti Polar Lipids Inc. (Alabaster, USA). All other chemicals were purchased from Carl Roth GmbH & Co KG (Karlsruhe, Germany), Fluka-Chemie AG (Buchs, Switzerland), Merck KGaA (Darmstadt, Germany) or Sigma-Aldrich Chemie GmbH (Deisenhofen, Germany) with the highest possible degree of purity.

2.2. Protein production and preparation

GCAP-2 was produced in a fed-batch fermentation process by heterologous expression in *Escherichia coli* BL21(DE3) carrying a pET-11a expression vector encoding for bovine GCAP-2 and the plasmid pBB131 encoding for the yeast N-myristoyl transferase I, enabling the bacterial cells to perform this eukaryotic post-translational modification [4,5,29]. As defined salt medium, a slightly modified version of the medium described in [30] was used. The final composition was 10 - 20 g glucose, 3.2 g/l NH_4Cl, 13.3 g/l KH_2PO_4, 4.3 g/l Na_2HPO_4, 1.2 g/l $MgSO_4 \cdot 7\ H_2O$, 1.7 g/l citrate $\cdot\ H_2O$, 8.4 mg/l EDTA, 2.5 mg/l $CoCl_2 \cdot 6\ H_2O$, 1.5 mg/l $CuCl_2 \cdot 2\ H_2O$, 3.0 mg/l H_3BO_3, 2.5 mg/l $Na_2MoO_4 \cdot 2\ H_2O$, 13.0 mg/l $Zn(CH_3COO)_2 \cdot 2\ H_2O$, 100.0 mg/l Fe(III)citrate $\cdot\ H_2O$ with a pH of 6.7, for ^{15}N-labeling $^{15}NH_4Cl$ was used and for ^{13}C-labeling, the citrate was omitted and uniformly ^{13}C-labeled glucose was used. The pH (6.7) and the temperature (37 °C) were kept constant during the entire fermentation process. The oxygen level was held above 30% and the foam production was suppressed by adding Antifoam 204. Glucose and NH_4Cl were fed as needed. Myristoylation was achieved by adding myristic acid (50-100 g/l in ethanol) to the growth medium (final concentration ~100 mg/l) 30 min before and after induction with IPTG. The cells were harvested by centrifugation (7459 RCF, 30 min, 4 °C) 4 h after induction. The biomass was resuspended (1 g wet-weight biomass / 10 ml buffer) in inclusion body buffer 1 (100 mM Tris/HCl pH 8.0, 1 mM EDTA) and after addition of 10 mg lysozyme for 1 h stirred and incubated on ice. The cells were then disrupted using a French-press (3 passages, 1000 bar) and afterwards incubated for 1 h at room temperature with 3 mM $MgCl_2$ and 10 mg DNase added. The inclusion bodies were separated by centrifugation (38420 RCF, 25 min, 4 °C) and then washed at least 2 times with inclusion body buffer 2 (100 mM Tris/HCl pH 7.0, 20 mM EDTA). They were afterwards incubated (1 g wet-weight / 10 ml buffer) for at least 2 h in solubilization buffer (100 mM Tris/HCl pH 8.0, 6 M guanidinium/HCl, 100 mM DTT, 1 mM EDTA) and so dissolved (final protein concentration 10 - 20 mg/ml). 10 ml of this mixture were then slowly dropped into 1 l of fast stirring ion exchange buffer (20 mM Tris/HCl pH 8.0, 1 mM $CaCl_2$, 1 mM DTT) and afterwards the solution was centrifuged (38420 RCF, 25 min, 4 °C) and filtered (cellulose nitrate filter from Satorius AG, Göttingen, Germany) to remove the precipitates. Then, the solution was loaded onto two HiTrap Q HP 5 ml ion-exchange columns (from Amersham Pharmacia Biotech, Freiburg, Germany) equilibrated with ion exchange buffer and the GCAP-2 was eluted by step elution (using the ion exchange buffer with 400 mM NaCl added). The protein solution was then dialyzed against storage buffer (20 mM Na_2HPO_4 pH 7.0, 1 mM DTT), frozen in liquid nitrogen and stored at -80 °C or diluted and directly used for reversed-phase HPLC to separate myristoylated from non-myristoylated GCAP-2. The VP 250/16 NUCLEOSIL 300-5 C18 column (from Macherey-Nagel, Düren, Germany) was first equilibrated (3.418 ml/min flow) to 99% deionised water (+0.1% TFA) and 1% acetonitril, then 4 ml of protein solution were loaded in 1.5 min onto the column and then eluted by a step to 41% acetonitril followed by a linear gradient of 6 min to 61% acetonitril and a final step to 100%

acetonitril. Non-myristoylated GCAP-2 (~23%) elutes at ~10.3 min and myristoylated (~77%) at ~11.5 min. The success of RP-HPLC was controlled by SDS-PAGE and MALDI-TOF mass spectrometry. The appropriate elution fractions were then lyophilized and afterwards redissolved by incubating and shaking for at least 2 h in solubilization buffer (max. 10 mg/ml) at room temperature. Then, the protein was refolded again, by slowly dropping 5 - 7.5 ml of this solution into 500 ml of fast stirring refolding buffer (100 mM Tris/HCl pH 8.0 - 8.5, 500 mM Na_2SO_4, 1 mM DTT, 0.1 mM $CaCl_2$) with a final protein concentration of 100 - 150 μg/ml. No precipitation was observed. Afterwards, the solution was concentrated below 50 ml by ultrafiltration (using a PLGC 10 kDa MWCO membrane from Millipore, Billerica, USA), extensively dialyzed against the final buffer (20 mM MES pH 6.0, 10 mM $CaCl_2$, 2 mM TCEP) and then concentrated by centrifugal ultrafiltration (using an Amicon ultra centrifugal filter device with 5 – 10 kDa MWCO from Millipore, Billerica, USA) to the final volume of 500 μl (with a protein concentration between 200 - 900 μM). Just before measuring, 25 μl of D_2O were added for the lock signal.

2.3. Preparation of bicelles

DMPC/DHPC bicelles with q = 0.25 [31] were prepared by mixing 33.4 mg of DMPC (1,2-dimyristoyl-*sn*-glycero-3-phosphocholine) with 96.3 mg of DHPC (1,2-diheptanoyl-*sn*-glycero-3-phosphocholine) and adding 500 μl of buffer (20 mM MES pH 6.0, 10 mM $CaCl_2$, 2 mM TCEP). The mixture was then incubated for 30 min at room temperature and mixed by vortexing. Afterwards the mixture was incubated on ice for 30 min and then, while gently shaking, incubated at 42 °C for again 30 min. This step was repeated at least 3 times until the solution was clear.

2.4. NMR spectroscopy and assignment

All NMR spectra were recorded on Bruker DRX 600 MHz and Avance III 600 MHz spectrometers (Bruker, Rheinstetten, Germany) using either a 5-mm-TBI or a 5-mm-TXI probehead with z-gradient. All ^{1}H-^{15}N HSQC spectra were recorded at 50 °C using the standard pulse program [32]. For each titration step a ^{1}H-^{15}N HSQC experiment, using a relaxation delay of 0.8 s and the following acquisition parameters, was recorded: for CHAPS titration (^{15}N: 192 data points, 61 ms acquisition; ^{1}H: 4096 data points, 213 ms acquisition), for DPC titration (^{15}N: 256 data points, 81 ms acquisition; ^{1}H: 4096 data points, 213 ms acquisition), for DMPC/DHPC titration (^{15}N: 128 data points, 41 ms acquisition; ^{1}H: 4096 data points, 213 ms acquisition). For the backbone assignment, standard HNCO, HN(CA)CO, HNCA, HN(CO)CA triple resonance 3D spectra [33] were recorded using a relaxation delay of 1 s and with the recommended values for the number of scans, data points, and acquisition times: HNCO (number of scans (NS): 16; ^{13}C: 169.5 - 178.5 ppm, 128 data points, 47 ms acquisition; ^{15}N: 106 - 132 ppm, 72 data points, 23 ms acquisition; ^{1}H: -3.5 - 12.5 ppm, 3072 data points, 160 ms acquisition), HN(CA)CO (NS: 32; ^{13}C: 169.5 - 178.5 ppm, 76 data points, 28 ms acquisition; ^{15}N: 106 - 132 ppm, 72 data points, 23 ms acquisition; ^{1}H: -3.4 - 12.6 ppm, 3072 data points, 160 ms acquisition), HNCA (NS: 16; ^{13}C: 36 - 68 ppm, 96 data points, 10 ms acquisition; ^{15}N: 106 - 132 ppm, 72 data points, 23 ms acquisition; ^{1}H: -3.2 - 12.8 ppm, 3072 data points, 160 ms acquisition), HN(CO)CA (NS: 24; ^{13}C: 36 - 68 ppm, 104 data points, 11 ms acquisition; ^{15}N: 106 - 132 ppm, 72 data points, 23 ms acquisition; ^{1}H: -3.2 - 12.8 ppm, 3072 data points, 160 ms acquisition).

For the titration experiments, a CHAPS, DPC, or bicelle stock solution was prepared in the same buffer as the protein sample, and stepwise titrated into the protein sample. As a measure for the structural influences of the titrated substance the weighted chemical shift difference Δδ [34] was calculated:

$$\Delta\delta = \sqrt{(\Delta\delta_H)^2 + (\Delta\delta_N/5)^2} \quad (1)$$

($\Delta\delta_X$: difference of chemical shift in the X dimension given in ppm). A difference of 0.02 ppm [35] or 0.04 ppm [36] is commonly considered as significant.

2.5. CS-ROSETTA modeling

The homology model of myristoylated Ca^{2+} bound GCAP-2 was constructed based on the crystal structure of GCAP-1 (PDB ID: 2R2I, [20]). It was then refined leveraging the measured back bone chemical shifts (H^N, N^H, C' and Cα) and using CS-ROSETTA [28,37]. Briefly: A total of 14,500 different models were created using a loop modeling approach and relaxation protocol. Loops ranged from residues 3-22, 34-40, 48-54, 119-145 and 189-203, excluding only the EF hand residues. Theoretical chemical shifts for all generated models were predicted using Sparta + [50] and the original CS-ROSETTA scoring function was used. A detailed protocol capture of the modeling process can be found in the supplementary information.

3. Results

3.1. Assignment and secondary structure of myristoylated GCAP-2

As a prerequisite for the investigation of the interaction of myristoylated GCAP-2 with lipid surfaces by solution-state NMR, we carried out the backbone assignment of the Ca^{2+}-bound myristoylated form of the protein. Because of the higher quality of the 3D triple resonance NMR spectra, the assignment was carried out at 50 °C and in the presence of 10 mM CHAPS. Under these conditions, we were able to assign ~84% of all backbone signals unambiguously. A ^{1}H-^{15}N HSQC NMR spectrum of myristoylated GCAP-2 with the signal assignments is shown in Fig. 1

Using TALOS + [37] the secondary structure of myristoylated GCAP-2 was predicted from the measured chemical shifts of the backbone signals (C^α, C', N^H, H^N). The result of this analysis is shown in Fig. 2. For comparison, the secondary structure of Ca^{2+}-bound non-myristoylated GCAP-2 [19] is also shown schematically. Similar to the non-myristoylated form and not surprisingly, myristoylated GCAP-2 shows four EF-hands. We could also identify the flexible loop comprising amino acids 129-146, which represents a main difference between GCAP-1 and GCAP-2. In addition, the termini of the protein were determined to be unstructured in the presence of 10 mM CHAPS. The N-terminus shows the only relevant difference between our secondary structure for the myristoylated form (determined from the backbone chemical shifts with TALOS+) and the secondary structure of non-myristoylated GCAP-2 (determined by [19]). In our preparation of myristoylated GCAP-2, we could not find any indication for the presence of the short N-terminal helix described in the literature [19]. Our result is also in agreement, with previous solid-state NMR investigations of a short membrane bound N-terminal peptide of GCAP-2, where this short helix could also not be confirmed [38].

3.2. Influence of the myristoyl moiety on the protein structure

Alterations in the chemical shifts (especially for $^{15}N^H$ and $^1H^N$) are a sensitive indicator for structural changes of a protein. We investigated the structural influence of the myristoyl moiety by comparing the chemical shifts of the backbone signals in the ^{1}H-^{15}N HSQC spectra of myristoylated and non-myristoylated GCAP-2 under the exact same buffer conditions (20 mM MES pH 6.0, 10 mM $CaCl_2$, 2 mM TCEP) and comparable protein concentrations (~250 μM). The NMR spectra are shown in Fig. S1. Because of the strong influence of the attachment of the myristoyl moiety on the chemical shift of many signals, a transfer of the assignment to the non-myristoylated form was unambiguous for only ~56% of all backbone signals. Fig. 3 shows the weighted chemical shift difference Δδ (see Eq. (1) [35,36]) between the myristoylated and the non-myristoylated forms of GCAP-2 as a measure for the

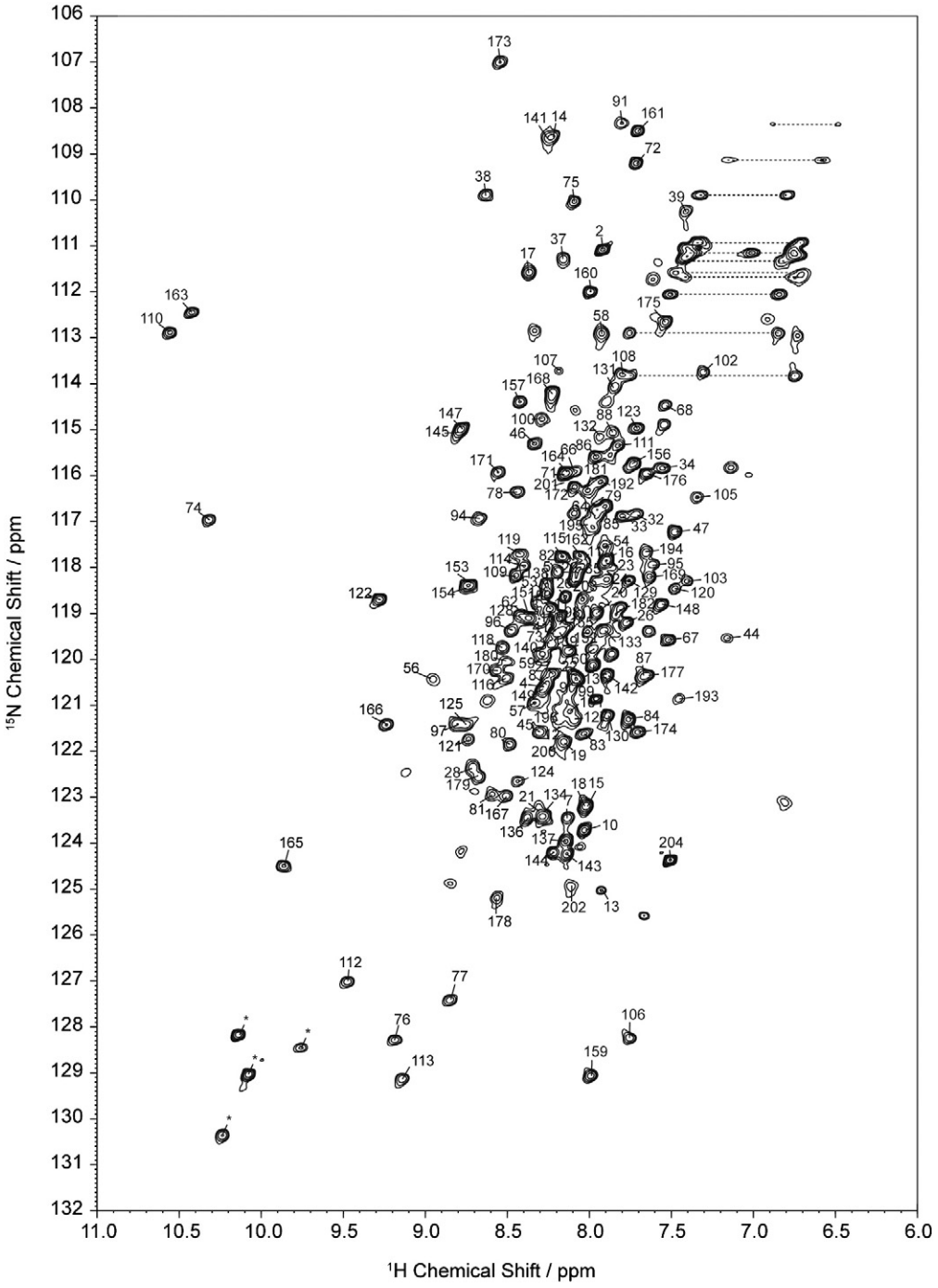

Fig. 1. ^{1}H-^{15} N HSQC spectrum of myristoylated GCAP-2 and assignment of ~84% of the backbone signals (by residue number). The sample contained 200 μM myristoylated GCAP-2 in 500 μl buffer (20 mM MES pH 6.0, 10 mM DTT, 10 mM $CaCl_2$, 10 mM CHAPS) with 25 μl D_2O added for the lock signal. Trp side chains signals are marked with an asterisk (*) and side chain signals arising from NH_2-groups are connected by dotted lines.

structural influence of the myristoyl moiety along the amino acid sequence. Overall, the influence of the myristoyl moiety is quiet strong. Nearly half of the signals (46.4%) change their chemical shift by more than 0.02 ppm and a change in chemical shift of more than 0.04 ppm is observed for 27.3% of the signals. The most significant chemical shift change is observed for Thr_{58}. The mean chemical shift difference for all assigned residues is 0.03 ppm. Nevertheless, the influence of the myristoyl moiety on the GCAP-2 chemical shifts is not evenly distributed. The presence or absence of the myristoyl chain shows the main structural influence in the N-terminal half of the protein at residues 44-58, at the end of the F-helix of the third EF hand and the following loop region at residues 120-134, and near the C-terminus of the protein, residues 175 – 194 (see Fig. 3).

3.3. Influence of CHAPS on the structure of myristoylated and non-myristoylated GCAP-2

GCAP-2 has a tendency to form oligomers at high concentration [39], which renders solution-state NMR spectroscopy difficult because the higher molecular weight and the dynamic equilibrium between the different oligomeric states cause a substantial signal broadening. Ames et al. used 25 mM octyl-β-D-glucopyranosid to prevent oligomer

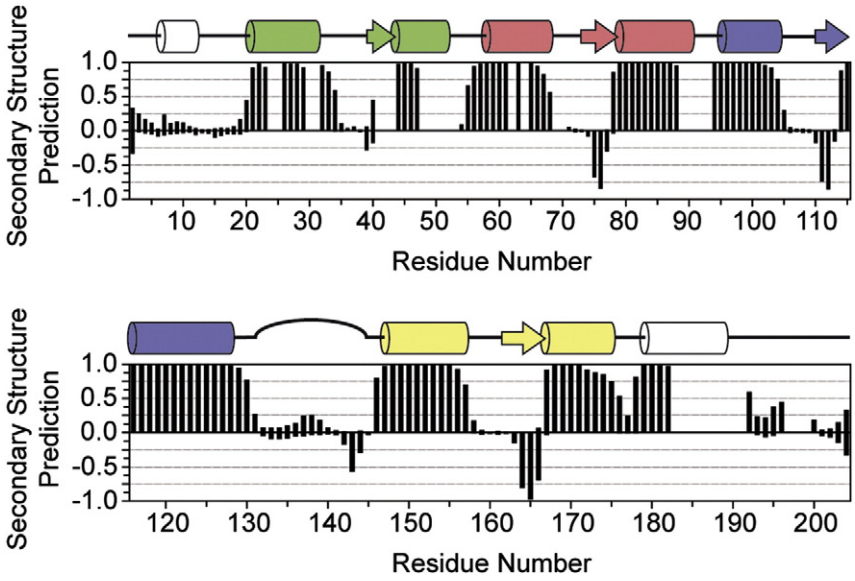

Fig. 2. Secondary structure of myristoylated GCAP-2 (in the presence of 10 mM CHAPS) based on the backbone chemical shifts (C^{α}, C', N^{H}, H^{N}) as predicted by TALOS+. A secondary structure prediction value of 1 means α-helical, -1 refers to β-strand and a score around 0 indicates a random-coil conformation. For comparison, the secondary structure of Ca^{2+}-bound non-myristoylated GCAP-2 according to literature is depicted above the graph [19]. Random-coil structures are depicted as lines, α-helices as cylinders and β-strands as arrows; the flexible loop, as a main difference to GCAP-1, is also highlighted. The different EF hand motives were consecutively color coded (EF-1: green, EF-2: red, EF-3: violet, EF-4: yellow).

formation and sharpen the NMR signals [19], which enabled them to solve the structure of non-myristoylated GCAP-2 [40]. For myristoylated GCAP-2, octyl-β-D-glucopyranosid had not such a positive effect on the NMR spectra (data not shown), however, a significant improvement of the NMR spectra could be obtained in the presence of CHAPS. CHAPS is a mild, non-denaturing detergent that prevents protein-protein interactions and therefore suppresses oligomerization [40,41]. CHAPS was also used for NMR investigations on the related protein recoverin [42]. Because our assignment of the myristoylated form of GCAP-2 was also done in the presence of CHAPS, we investigated the structural influence of CHAPS on the myristoylated as well as on the non-myristoylated form. ^{1}H-^{15}N HSQC spectra of both forms of the protein show significant differences for varying CHAPS concentrations (Fig. S2). Fig. 4 shows the weighted chemical shift difference Δδ along the protein amino acid sequence during the CHAPS titration for the myristoylated form of GCAP-2. For comparison, the chemical shift perturbations upon CHAPS addition of the non-myristoylated form of GCAP-2 is shown in Fig. S3. Overall, the influence of CHAPS on the myristoylated form (Fig. 4) is

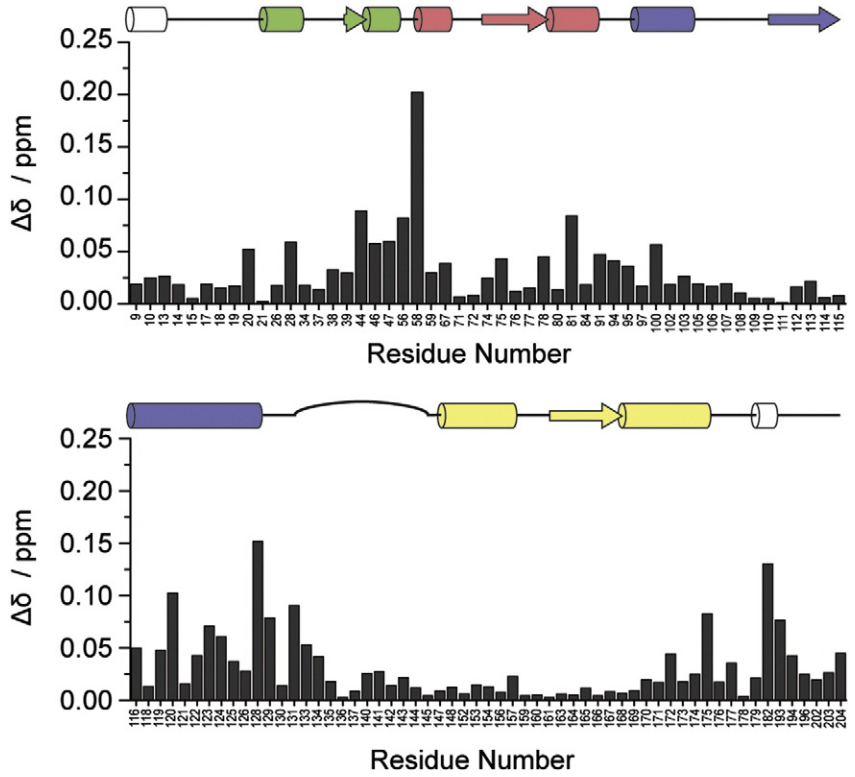

Fig. 3. Weighted chemical shift differences Δδ between the myristoylated and the non-myristoylated forms of GCAP-2 as a measure for the structural influence of the myristoyl moiety in the absence of detergent or lipid. For comparison, the secondary structure of Ca^{2+}-bound non-myristoylated GCAP-2 according to literature is depicted schematically above the graph [19].

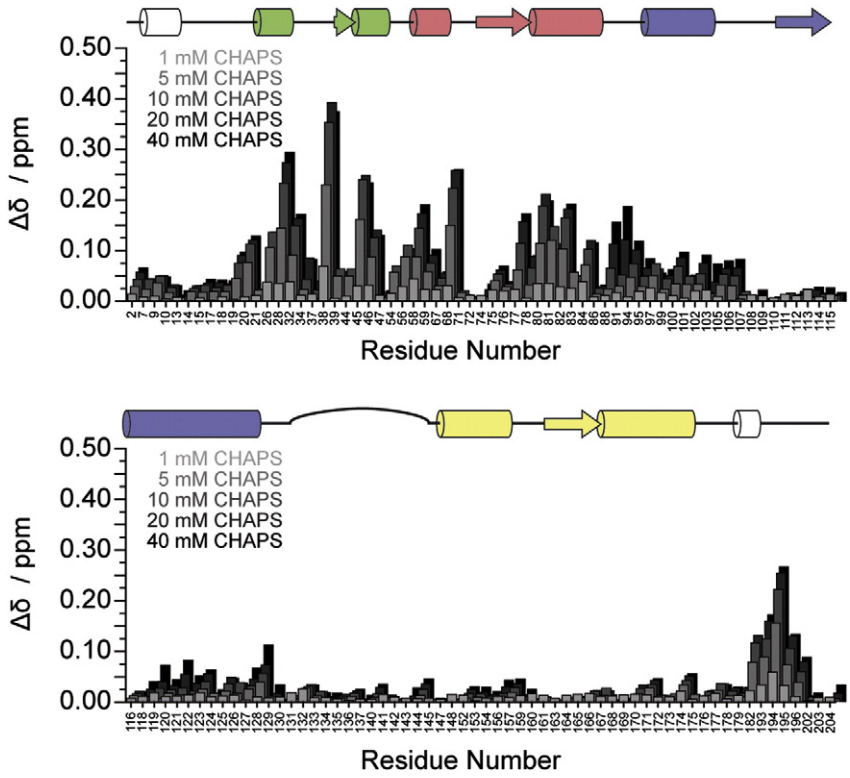

Fig. 4. Influence of increasing CHAPS concentration on the weighted chemical shift differences Δδ of myristoylated GCAP-2, measured in the ^{1}H-^{15} N HSQC spectra as a function of CHAPS concentration. For comparison, the secondary structure of Ca^{2+}-bound non-myristoylated GCAP-2 according to literature is depicted schematically above the graph [19].

quite strong and even stronger than the influence of the myristoyl moiety, but as the dispersion of the signals in ^{1}H-^{15} N HSQC spectra (Fig. S2) shows, it is clearly not denaturing the protein. However, quite strong chemical shift changes are observed. For 74.4% of the signals, the chemical shifts changes more than 0.02 ppm and almost half of the signals (48.0%) shift by more than 0.04 ppm. The most significant chemical shift change is observed for Gly_{38}. The mean chemical shift difference for all residues between the first and the last titration point is 0.06 ppm. Interestingly, most chemical shift alterations are observed in the N-terminal half of the protein, while the C-terminal half only shows moderate chemical shift changes except for the terminal ~20 amino acids. This pattern is particularly pronounced for the myristoylated form of GCAP-2. Interestingly, a similar pattern of influenced amino acids was observed for the comparison of the myristoylated and non-myristoylated forms of the protein, in particular for the N-terminal half of the molecule (Fig. 3). Only the influence at the F-helix of the third EF-hand is far less pronounced compared to the influence of the myristoyl moiety onto the same region (see Fig. 3).

CHAPS also caused a structural influence on the non-myristoylated form (Fig. S3). Again, a similar distribution of influenced amino acids is observed, but overall the chemical shift changes are less pronounced. To determine the myristoylation specific effect of CHAPS, we calculated the absolute difference (ΔΔδ) between the weighted chemical shift difference of the myristoylated and non-myristoylated form: $\Delta\Delta\delta = |\Delta\delta_{myr.} - \Delta\delta_{non-myr.}|$. The result is shown in Fig. S4. The myristoylation specific influence of CHAPS shows a similar pattern as observed for attaching the myristoyl moiety. Moreover the strength of the effect is also comparable.

3.4. Influence of DPC on the structure of myristoylated and non-myristoylated GCAP-2

Because CHAPS does not represent a good membrane mimicking detergent [43], in the next step, we tested the structural influence of DPC micelles on GCAP-2. DPC forms micelles that provide surfaces, which better resemble those of phospholipid membranes than CHAPS. DPC features a physiological phosphocholine head group as one of the main phospholipids of the cellular membrane and it is widely used in solution-state NMR investigations on membrane proteins [44].

The ^{1}H-^{15} N HSQC spectra of myristoylated GCAP-2 in the absence and presence of 40 mM DPC are shown in Fig. S5. As a general impression, the chemical shift dispersion of the NMR signals is markedly reduced in the presence of 40 mM DPC. As a consequence, only ~37% of the signals could be assigned. The weighted chemical shift differences Δδ along the protein amino acid sequence as a function of increasing DPC concentrations for the myristoylated GCAP-2 is shown in Fig. 5. As seen from these titrations, DPC causes very strong effects, especially at higher concentrations (>5 mM). In contrast to the CHAPS titration, the influence of DPC appears to extend over the entire protein sequence. The mean chemical shift difference for all residues is 0.17 ppm. As the dispersion of the ^{1}H-^{15} N HSQC signals shows (see Fig. S5), DPC has a denaturing effect on GCAP-2. It is a bit surprising that we observed such an effect for DPC here, which is known to be a relatively well-suited membrane mimicking detergent. The denaturing effect, we observed could be related to the fact that GCAP is not a membrane protein with stable transmembrane segments, but rather a relatively unstable soluble protein, that may get more unstable in the presence of the DPC surfaces.

3.5. Influence of bicelles on the structure of myristoylated and non-myristoylated GCAP-2

Finally, we investigated the structural changes upon binding of myristoylated GCAP-2 on DMPC/DHPC bicelles (q = 0.25), as the most membrane-like structure applicable to solution-state NMR. Fig. S6 shows the superposition of the ^{1}H-^{15} N HSQC spectra in the absence and in the presence of bicelles (10 mM DMPC / 40 mM DHPC). While there are significant chemical shift changes, the overall chemical shift dispersion remains comparable in the presence and in the absence of DMPC/DHPC bicelles. In Fig. 6, the weighted chemical shift difference

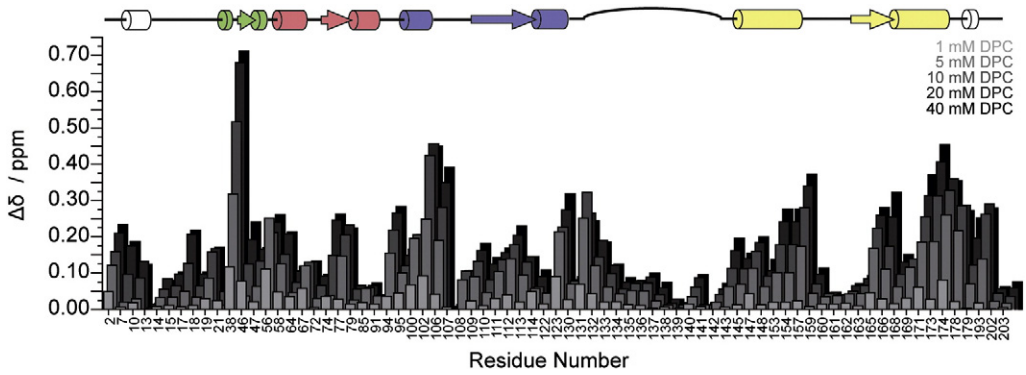

Fig. 5. Influence of DPC on myristoylated GCAP-2, measured as the weighted chemical shift difference Δδ in the ^{1}H-^{15}N HSQC spectra. For comparison, the secondary structure of Ca^{2+}-bound non-myristoylated GCAP-2 is depicted schematically above the graph [19].

Δδ along the amino acid sequence of myristoylated GCAP-2 is plotted. DMPC/DHPC bicelles cause a weaker effect then CHAPS and DPC. The mean chemical shift difference between the first and the last titration point is 0.04 ppm at the largest bicelle concentration. Nevertheless, DMPC/DHPC bicelles cause a structural effect with a similar pattern as CHAPS, so the main chemical shift alterations are observed in the N-terminal half of the protein, the F-helix of the third EF-hand, and near the C-terminus (see Fig. 6). Compared to the effect of the myristoyl moiety alone (see Fig. 3), bicelles cause a more pronounced (nearly doubled) and wider but more evenly distributed effect in the N-terminal half of the protein, at the F-helix of the third EF-hand, and near the C-terminus the effect is of comparable strength. Compared with the effect of CHAPS on the myristoylated form, the effect on the N-terminal region is wider, more evenly distributed but comparable in strength. The effect at the F-helix of the third EF-hand has, in the case of bicelles, a broader distribution and is slightly stronger; at the C-terminus the distribution is again broader but also weaker compared to the effect of CHAPS.

3.6. CS-ROSETTA homology model of myristoylated, Ca^{2+}-bound GCAP-2

We calculated a homology model for myristoylated GCAP-2 (Fig. 7b) based on the measured backbone chemical shifts (H^N, N^H, C' and Cα) for myristoylated GCAP-2 in the absence of membrane mimetics and based on the crystal structure of myristoylated, Ca^{2+}-bound GCAP-1. The RMSD of Cα back bone atom positions compared to the best scored model vs. the CS-ROSETTA score of each model is shown in Fig S7. The calculations based on the chemical shifts converged to a cluster with a radius of about 3 Å. At this point, it should be mentioned, that this special case of a myristoylated, Ca^{2+} binding protein poses a major challenge to CS-ROSETTA. Despite the fact that it is not a small protein (203 amino acids) and it is predominantly α-helical, the main challenge in the CS-ROSETTA protocol is accurate chemical shift prediction. To our knowledge no chemical shift prediction algorithm accounts for the chemical shift influences caused by the positive charges of the Ca^{2+} ions or even by the hydrophobicity of the myristic acid itself. This

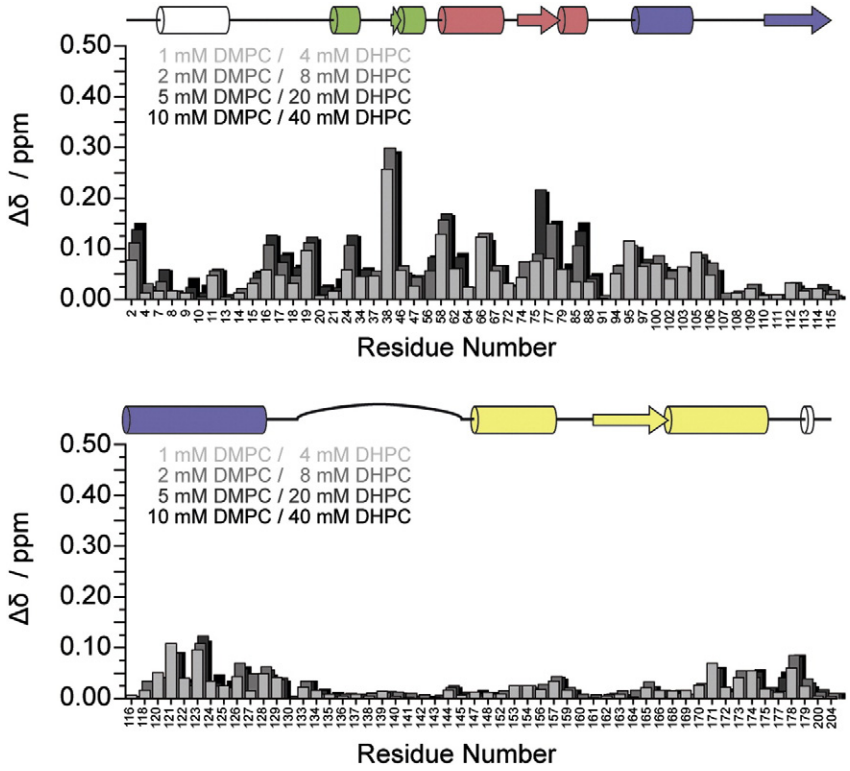

Fig. 6. Influence of DMPC/DHPC bicelles (q = 0.25) on myristoylated GCAP-2, measured as the weighted chemical shift difference Δδ in the ^{1}H-^{15}N HSQC spectra. For comparison, the secondary structure of Ca^{2+}-bound non-myristoylated GCAP-2 is depicted schematically above the graph [19].

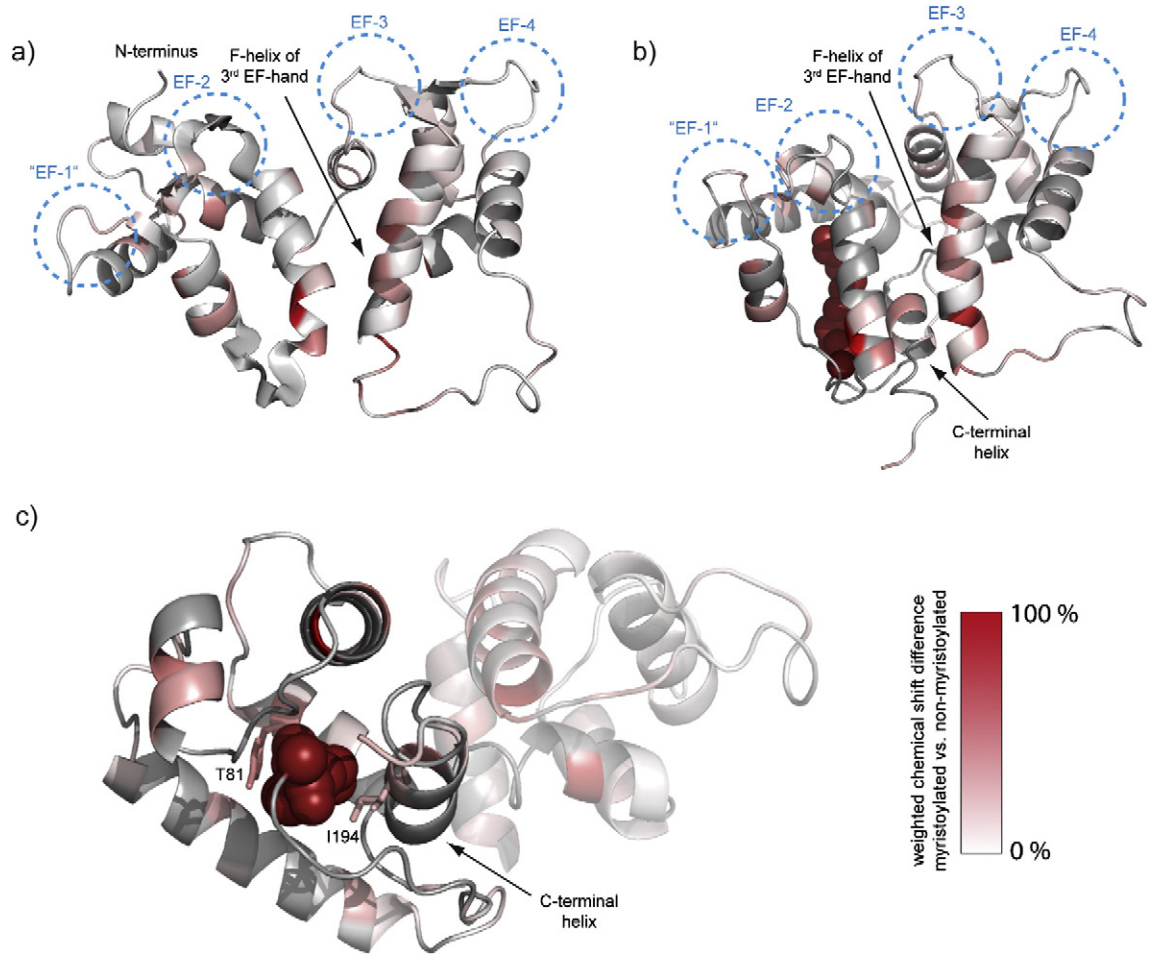

Fig. 7. Visualization of the observed ^{1}H and ^{15}N chemical shift changes between myristoylated and non-myristoylated GCAP-2 mapped onto the available NMR structure of non-myristoylated GCAP-2 (a) (PDB ID: 1JBA, [19]) and our CS-ROSETTA homology model of myristoylated GCAP-2 (b) based on the crystal structure of myristoylated GCAP-1 (PDB ID: 2R2I, [20]) and the measured backbone chemical shifts of myristoylated GCAP-2. A close-up look into the hydrophobic pocket, accommodating the myristoyl moiety is given in panel (c). The weighted chemical shift differences are linearly color coded in red, given relative to the maximal found chemical shift difference. Bound Ca^{2+} ions are not shown for clarity.

introduces a deviation between predicted and experimental chemical shifts which will be reflected in a wider and possibly biased structural ensemble. Consequently, the agreement between predicted and experimental chemical shift can be improved when ignoring the EF hand residues when scoring chemical shift agreement. As a result the structural ensemble gets more focused as expressed by a reduction in average RMSD to the best scoring model (see Fig. S7). Therefore, to calculate a structure of myristoylated, Ca^{2+}-bound GCAP-2 from chemical shifts only represents a major challenge. Nevertheless, Fig. S7 shows a convergence of the calculations and the best scored structure can be used as a first model of myristoylated, Ca^{2+} bound GCAP-2.

The calculated model showed some interesting features. First, the myristic moiety is locked into an N-terminal hydrophobic pocket. The relevant side chains that were found to interact with myristic acid in the crystal structure of GCAP-1 are also in close contact with the myristic acid in this model. The F-helix of the 3rd EF-hand is still bended but not kinked as much as in the crystal structure of GCAP-1 but more than in the crystal structure of non-myristoylated GCAP-3. The C-terminus, although loop modeled, contains an α-helix which again forms an important part of the myristoyl moiety binding pocket.

4. Discussion

While protein lipid modifications are classical membrane anchors [45], experimental results have so far not unambiguously explained the role of the N-myristoylation of GCAP-2. The most troublesome experimental observation is the fact that the membrane binding energy for myristoylated and non-myristoylated GCAP-2 is approximately the same [22] while thorough thermodynamic considerations [23] one would predict a difference in ΔG^0 of about -30 kJ/mol between the two forms of the protein, which was clearly not observed. This would allow the conclusion that the myristoyl moiety of GCAP-2 does not function as a membrane anchor. Such a scenario would be in agreement with the crystal structure of GCAP-1 [20], which showed that the myristoyl chain is buried within the protein to exert a structure stabilizing function [46]. In contrast, ^{2}H NMR results have clearly shown that the myristoyl moiety is membrane inserted when GCAP-2 is bound to lipid bilayers [27]. This seems to suggest that in the absence of any membranes, the myristoyl moiety of GCAP-2 could indeed be buried inside the protein but is released from the protein interior and inserted into the membrane when the protein senses the low dielectric constant environment of the bilayer surface. It has also been suggested that the membrane orientation of the myristoylated and non-myristoylated protein may be different giving rise to the low differences in ΔG^0 for membrane binding of GCAP-2 in the presence or absence of the myristoyl anchor [27]. Nevertheless, a myristoyl switch of some kind would be required for such a model and the goal of this study was to investigate what structural alterations accompany the transfer of GCAP-2 from the aqueous state to the membrane bound conformation. To this end, we determined a structural model of myristoylated GCAP-2 on the basis of NMR chemical shifts in solution and investigated (*i*) structural differences between the myristoylated and non-myristoylated

GCAP-2 in solution and (*ii*) structural changes of the protein in the presence of detergents and membrane mimetics by solution state NMR spectroscopy.

4.1. Structural differences between the myristoylated and non-myristoylated GCAP-2

The presence and absence of the myristoyl chain on GCAP-2 showed significant chemical shift changes in the protein that are mostly localized in the first and second EF hands, the F helix of the third EF hand, the beginning of the loop to the fourth EF hand, and the C-terminal end of the protein (Fig. 3). However, as the TALOS + analysis has shown, the presence or absence of the myristoyl moiety has no relevant influence on the general secondary structure of GCAP-2. The observed changes could be attributed to either local effects or also more global tertiary structure changes of the protein. This particularly concerns the N-terminal half of the molecule. These chemical shift differences between the myristoylated and non-myristoylated forms of the protein are unlikely to stem from a water exposed myristoyl chain attached to the flexible N-terminus. Therefore, our results are in agreement with the localization of the myristoyl moiety inside the protein in the absence of any membrane or membrane mimic. This can be rationalized by comparison with literature data: the FCaBP is a protein with a solvent exposed myristoyl moiety and the ^{1}H-^{15} N HSQC spectra of the myristoylated form and the non-myristoylated form show virtually no differences [47]. Therefore, the rather drastic chemical shift changes observed for GCAP-2 suggest that the myristoyl moiety of GCAP-2 should be bound to the protein in a surface pocket or buried inside the hydrophobic core of the molecule.

To understand the localization of the myristoyl chain in relation to the observed chemical shift changes, we map the chemical shift changes onto the 3D structure of non-myristoylated GCAP-2 and onto the CS-ROSETTA model of myristoylated GCAP-2 (see 3.6, Fig. 7a and b). It can be seen, that the myristoyl moiety of GCAP-2 localizes in a hydrophobic pocket in the N-terminal part of the protein forming close contact to mostly the same amino acids, which constitute the hydrophobic myristic acid binding pocket in the crystal structure of GCAP-1 [20]. Stephen et al. indentified a set of hydrophobic and aromatic amino acids in close contact to the myristoyl moiety [20]. Indeed, the same residues display strong chemical shift differences caused by the myristoyl moiety in GCAP-2, in the cases where unambiguous assignment transfer was possible and (see Fig. 7c). Furthermore, the authors emphasize the important role of the C-terminal helix of GCAP-1 for the binding pocket for the myristoyl moiety [20]. Indeed, we also find strong chemical shifts differences in this part caused by the myristoyl moiety and the model of myristoylated GCAP-2 also suggests that the C-terminal helix is part of the myristic acid binding pocket. Most likely the myristoyl moiety of free GCAP-2 is bound to the protein and buried inside a hydrophobic pocket similar to the arrangement shown in the crystal structure of GCAP-1.

Interestingly, one of the major influences of the myristoyl moiety on the structure of GCAP-2 is found in the F-helix of the third EF-hand, and compared to the solution-NMR structure of non-myristoylated GCAP-2, the CS-ROSETTA model of myristoylated GCAP-2 shows that this helix is bent, additionally this helix is strongly kinked in the crystal structure of myristoylated GCAP-1, but straight in the crystal structure of non-myristoylated GCAP-3. This raises the question, if the kink is caused by the myristoylation and if it also exists in myristoylated GCAP-2. The kink is localized around residue Ile_{123}, and indeed, this region shows significant chemical shift changes (see Fig. 3). Thus, it is plausible that the presence of the myristoylation also induces a structural change in F-helix of the third EF-hand. We have tried to determine chain NOEs in that region; however, given the very crowded situation of the predominantly α-helical protein (see Fig. 1), it was in our hands not possible to assign a sufficient amount of side chain signals for a detailed NOE analysis. Therefore, without further structural data, we cannot substantiate structural details of any conformational change in this region. Kollmann et al. [48] investigated the effect of myristoylation and Ca^{2+} binding onto the fluorescence lifetime and rotational anisotropy of the fluorescence dye Alexa647 attached to Cys_{111} (at the beginning of the F-helix of the third EF-hand) and Cys_{131} (at the end of the F-helix of the third EF-hand) of GCAP-2. In agreement with our data, they also found an influence of the myristoylation onto this part of the protein.

The observed chemical shift differences between the myristoylated and non-myristoylated forms of GCAP-2 also suggest a second structural change to occur in the beginning of the E-helix of the second EF hand. While the NMR structure of non-myristoylated GCAP-2 shows this region relatively poorly structured with a kink in the helix, in the crystal structure of GCAP-1 this helix is straight and well structured. Indeed, we find the largest chemical shift change exactly in this region (around Thr_{58}), suggesting that the addition of the myristoyl moiety leads to a structuring of this region as the homology model suggests.

Taken together, the chemical shift data suggest that the addition of the myristoyl chain to GCAP-2 leads to significant structural alterations and the chemical shift changes observed are in agreement with a conformation, where the myristoyl moiety is buried inside the protein similar to the crystal structure of GCAP-1 [20].

4.2. Structural changes of GCAP-2 upon binding to lipophilic surfaces

To reconcile this structural model with the previous experimental observation that the myristoyl chain of GCAP-2 is bilayer inserted when the protein is bound to lipid membranes, we investigated structural changes in the myristoylated protein in the presence of membrane mimetics CHAPS micelles, DPC micelles, and DMPC/DHPC bicelles. While the chemical shift differences and the accompanied structural changes of myristoylated GCAP-2 caused by CHAPS micelles and DMPC/DHPC bicelles showed a clear pattern, the presence of DPC micelles lead to rather homogeneous chemical shift changes. This suggests that the structural changes caused by DPC micelles are more or less evenly distributed along the entire protein sequence. This strong effect of DPC on the GCAP-2 structure is apparently caused by the denaturing effect of this detergent, which could be seen by the loss of signal dispersion in the ^{1}H-^{15} N HSQC spectra during the DPC titration (see Fig. S5). In contrast, CHAPS micelles and DMPC/DHPC bicelles induced strong chemical shift alterations of GCAP-2 following a clear pattern and evidently no denaturing effect was observed.

To visualize the changes caused by CHAPS micelles and DMPC/DHPC bicelles we again plot the chemical shift changes caused by those agents onto the CS-ROSETTA model of myristoylated GCAP-2 as shown in Fig. 8. The protein structure changes, due to the interaction with these membrane mimics, mostly in the N-terminal part, but also at the C-terminus and in the F-helix of the third EF-hand.

It should be noted that the chemical shift changes caused by the membrane mimetics does not resemble the reversed effect caused by the intrusion of the myristoyl moiety into the hydrophobic pocket. But it cannot be ignored that all variations of the environment cause chemical shift changes not only the differences in the localization of the myristoyl group but also the increasing amount of detergent or bicelles in the sample. Furthermore, after binding, some of the influenced residues may experience even stronger chemical shift change then others, due to the higher local concentration of lipids or because they are directly involved in the binding action.

However, the patterns of chemical shift changes very closely resemble the chemical shift differences between myristoylated and non-myristoylated GCAP-2. It is therefore tempting to suggest that these chemical shift changes indicate the translocation of the myristoyl moiety from the protein interior into the hydrophobic environment of the membrane mimetic. This can explain why the myristoyl chain of GCAP-2 is always found membrane embedded in membrane-associated GCAP-2 [22,27,38]. Such a scenario could be interpreted as a myristoyl

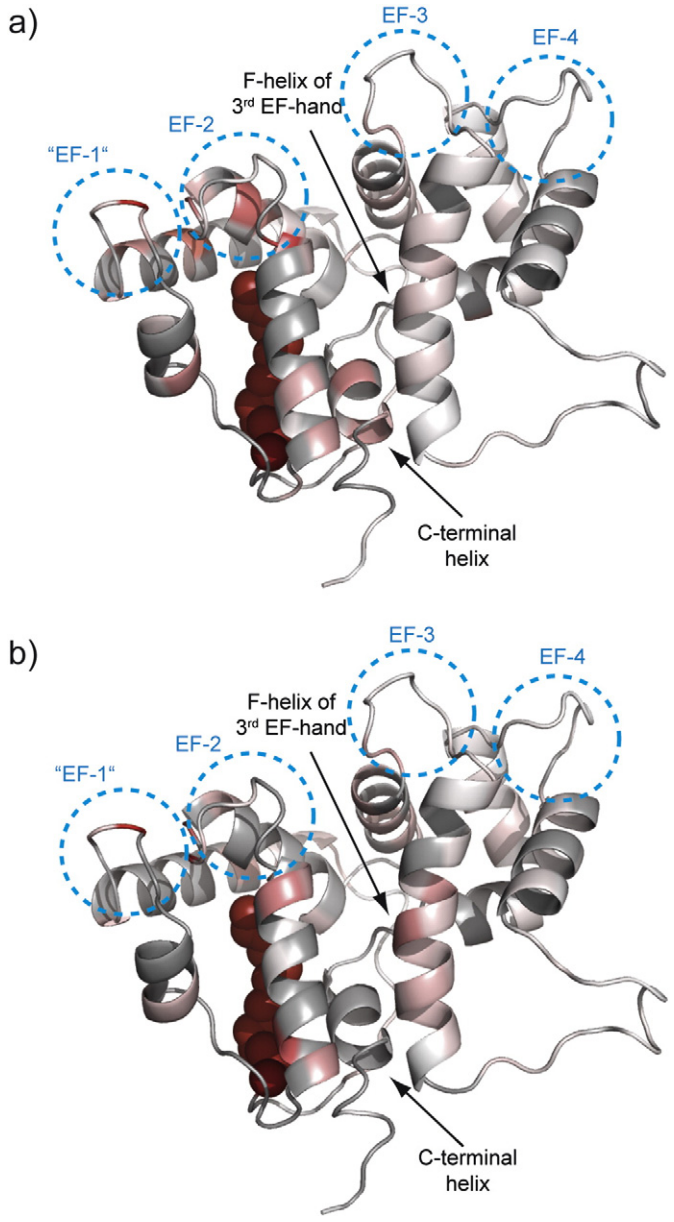

Fig. 8. Visualization of the influence of CHAPS micelles (20 mM CHAPS) (a) and DMPC/DHPC bicelles (10 mM DMPC / 40 mM DHPC) (b) on the observed ^{1}H and ^{15}N chemical shift changes of myristoylated GCAP-2. The chemical shift changes are linearly color coded in red mapped onto our CS-ROSETTA homology model of myristoylated GCAP-2 based on the crystal structure of myristoylated GCAP-1 (PDB ID: 2R2I, [20]) and the measured backbone chemical shifts of myristoylated GCAP-2. Bound Ca^{2+} ions are not shown for clarity.

switch mechanism induced by the presence of membrane(-like) structures.

For both CHAPS micelles and DMPC/DHPC bicelles, the biggest chemical shift difference experiences Gly_{38}, which is located in the loop region of the 1st EF-hand. Due to a Cys-Pro sequence, the first EF-hand is not able to bind Ca^{2+} [19]. Because glycine lacks a sterically hindering side chain, it can easily adopt different backbone torsion angles [49], therefore, one can speculate if it may serve as hinge for the myristoyl moiety switch mechanism.

5. Conclusions

The myristoyl moiety of GCAP-2 causes significant structural changes of the protein. All NMR results obtained here support the view that the myristoyl moiety is buried inside the protein in the absence of membranes or micelles as depicted in Figs. 7 and 8. The titration of CHAPS micelles and DMPC/DHPC bicelles cause chemical shift differences in the same regions of the protein, which also differ between the myristoylated and non-myristoylated forms of GCAP-2. Therefore, it is plausible that the presence of membranes or micelles induces a conformational switch, which causes the myristoyl chain to be released from the hydrophobic protein interior to insert into the hydrophobic core of the membrane without much change in the free energy. Such a model would be in agreement with the experimental observations that (*i*) the myristoyl chain is always found membrane inserted in the presence of membranes [27], and (*ii*) no major differences in ΔG^0 are observed for membrane binding of myristoylated and non-myristoylated GCAP-2 [22].

Acknowledgements

The project was supported by a grant from the DFG (HU 720/10-1). A.M. thanks the Serbian Ministry of Education, Science and Technological Development for a grant (project number 172048). S.T. is grateful for support from the Vanderbilt Leipzig Exchange program.

Appendix A. Supplementary data

Supplementary data to this article can be found online at http://dx.doi.org/10.1016/j.bbamem.2014.07.012.

References

[1] A.M. Dizhoor, J.B. Hurley, Regulation of photoreceptor membrane guanylyl cyclases by guanylyl cyclase activator proteins, Methods 19 (1999) 521–531.
[2] F. Haeseleer, Y. Imanishi, I. Sokal, S. Filipek, K. Palczewski, Calcium-binding proteins: intracellular sensors from the calmodulin superfamily, Biochem. Biophys. Res. Commun. 290 (2002) 615–623.
[3] J.C. Demar, D.R. Rundle, T.G. Wensel, R.E. Anderson, Heterogeneous N-terminal acylation of retinal proteins, Prog. Lipid Res. 38 (1999) 49–90.
[4] J.Y. Hwang, K.W. Koch, The myristoylation of the neuronal Ca^{2+}-sensors guanylate cyclase-activating protein 1 and 2, Biochim. Biophys. Acta 1600 (2002) 111–117.
[5] J.Y. Hwang, K.W. Koch, Calcium- and myristoyl-dependent properties of guanylate cyclase-activating protein-1 and protein-2, Biochemistry 41 (2002) 13021–13028.
[6] E.V. Olshevskaya, R.E. Hughes, J.B. Hurley, A.M. Dizhoor, Calcium binding, but not a calcium-myristoyl switch, controls the ability of guanylyl cyclase-activating protein GCAP-2 to regulate photoreceptor guanylyl cyclase, J. Biol. Chem. 272 (1997) 14327–14333.
[7] M. Chow, J.F. Newman, D. Filman, J.M. Hogle, D.J. Rowlands, F. Brown, Myristylation of picornavirus capsid protein VP4 and its structural significance, Nature 327 (1987) 482–486.
[8] J. Zheng, D.R. Knighton, N.H. Xuong, S.S. Taylor, J.M. Sowadski, L.F. Ten Eyck, Crystal structures of the myristylated catalytic subunit of cAMP-dependent protein kinase reveal open and closed conformations, Protein Sci. 2 (1993) 1559–1573.
[9] L. Brunsveld, H. Waldmann, D. Huster, Membrane binding of lipidated Ras peptides and proteins — The structural point of view, Biochim. Biophys. Acta 1788 (2009) 273–288.
[10] M.D. Resh, Fatty acylation of proteins: new insights into membrane targeting of myristoylated and palmitoylated proteins, Biochim. Biophys. Acta 1451 (1999) 1–16.
[11] J.A. Boutin, Myristoylation, Cell. Signal. 9 (1997) 15–35.
[12] S. Zozulya, L. Stryer, Calcium-myristoyl protein switch, Proc. Natl. Acad. Sci. U. S. A. 89 (1992) 11569–11573.
[13] D. Ladant, Calcium and membrane-binding properties of bovine neurocalcin-delta expressed in Escherichia coli, J. Biol. Chem. 270 (1995) 3179–3185.
[14] M. Kobayashi, K. Takamatsu, S. Saitoh, T. Noguchi, Myristoylation of hippocalcin is linked to its calcium-dependent membrane association properties, J. Biol. Chem. 268 (1993) 18898–18904.
[15] J.B. Ames, R. Ishima, T. Tanaka, J.I. Gordon, L. Stryer, M. Ikura, Molecular mechanics of calcium-myristoyl switches, Nature 389 (1997) 198–202.
[16] T. Tanaka, J.B. Ames, T.S. Harvey, L. Stryer, M. Ikura, Sequestration of the membrane-targeting myristoyl group of recoverin in the calcium-free state, Nature 376 (1995) 444–447.
[17] K.G. Valentine, M.F. Mesleh, S.J. Opella, M. Ikura, J.B. Ames, Structure, topology, and dynamics of myristoylated recoverin bound to phospholipid bilayers, Biochemistry 42 (2003) 6333–6340.
[18] J.B. Ames, T. Tanaka, L. Stryer, M. Ikura, Portrait of a myristoyl switch protein, Curr. Opin. Struct. Biol. 6 (1996) 432–438.
[19] J.B. Ames, A.M. Dizhoor, M. Ikura, K. Palczewski, L. Stryer, Three-dimensional structure of guanylyl cyclase activating protein-2, a calcium-sensitive modulator of photoreceptor guanylyl cyclases, J. Biol. Chem. 274 (1999) 19329–19337.

[20] R. Stephen, G. Bereta, M. Golczak, K. Palczewski, M.C. Sousa, Stabilizing function for myristoyl group revealed by the crystal structure of a neuronal calcium sensor, guanylate cyclase-activating protein 1, Structure 15 (2007) 1392–1402.
[21] R. Stephen, K. Paiczewski, M.C. Sousa, The crystal structure of GCAP3 suggests molecular mechanism of GCAP-linked cone dystrophies, J. Mol. Biol. 359 (2006) 266–275.
[22] A. Vogel, T. Schröder, C. Lange, D. Huster, Characterization of the myristoyl lipid modification of membrane-bound GCAP-2 by ^{2}H solid-state NMR spectroscopy, Biochim. Biophys. Acta 1768 (2007) 3171–3181.
[23] K. Weise, D. Huster, S. Kapoor, G. Triola, H. Waldmann, R. Winter, Gibbs energy determinants of lipoprotein insertion into lipid membranes: the case study of Ras proteins, Faraday Discuss. 161 (2013) 549–561.
[24] A. Vogel, C.P. Katzka, H. Waldmann, K. Arnold, M.F. Brown, D. Huster, Lipid modifications of a ras peptide exhibit altered packing and mobility versus host membrane as detected by ^{2}H solid-state NMR, J. Am. Chem. Soc. 127 (2005) 12263–12272.
[25] D.W. O'Callaghan, R.D. Burgoyne, Identification of residues that determine the absence of a Ca^{2+}/myristoyl switch in neuronal calcium sensor-1, J. Biol. Chem. 279 (2004) 14347–14354.
[26] R.E. Hughes, P.S. Brzovic, A.M. Dizhoor, R.E. Klevit, J.B. Hurley, Ca^{2+}-dependent conformational changes in bovine GCAP-2, Protein Sci. 7 (1998) 2675–2680.
[27] S. Theisgen, L. Thomas, T. Schroder, C. Lange, M. Kovermann, J. Balbach, D. Huster, The presence of membranes or micelles induces structural changes of the myristoylated guanylate-cyclase activating protein-2, Eur. Biophys. J. 40 (2011) 565–576.
[28] Y. Shen, O. Lange, F. Delaglio, P. Rossi, J.M. Aramini, G. Liu, A. Eletsky, Y. Wu, K.K. Singarapu, A. Lemak, A. Ignatchenko, C.H. Arrowsmith, T. Szyperski, G.T. Montelione, D. Baker, A. Bax, Consistent blind protein structure generation from NMR chemical shift data, Proc. Natl. Acad. Sci. U. S. A. 105 (2008) 4685–4690.
[29] R.J. Duronio, E. Jackson-Machelski, R.O. Heuckeroth, P.O. Olins, C.S. Devine, W. Yonemoto, L.W. Slice, S.S. Taylor, J.I. Gordon, Protein N-myristoylation in Escherichia coli: reconstitution of a eukaryotic protein modification in bacteria, Proc. Natl. Acad. Sci. U. S. A. 87 (1990) 1506–1510.
[30] D.J. Korz, U. Rinas, K. Hellmuth, E.A. Sanders, W.D. Deckwer, Simple fed-batch technique for high cell density cultivation of Escherichia coli, J. Biotechnol. 39 (1995) 59–65.
[31] C.R. Sanders, J.P. Schwonek, Characterization of magnetically oriented bilayers in mixtures of dihexanoylphosphatidylcholine and dimyristoylphosphtidylcholine by solid-state NMR, Biochemistry 31 (1992) 8898–8905.
[32] S. Mori, C. Abeygunawardana, M.O. Johnson, P.C.M. Vanzijl, Improved sensitivity of HSQC spectra of exchanging protons at short Interscan delays using a new fast HSQC (FHSQC) detection scheme that avoids water saturation, J. Magn. Reson. B 108 (1995) 94–98.
[33] H. Oschkinat, T. Müller, T. Dieckmann, Protein structure determination with three- and four-dimensional NMR spectroscopy, Angew. Chem. Int. Ed. 33 (1994) 277–293.
[34] E.S. Seo, B.S. Blaum, T. Vargues, Cecco M. De, J.A. Deakin, M. Lyon, P.E. Barran, D.J. Campopiano, D. Uhrin, Interaction of Human beta-Defensin 2 (HBD2) with Glycosaminoglycans, Biochemistry 49 (2010) 10486–10495.
[35] D. Schlorke, L. Thomas, S.A. Samsonov, D. Huster, J. Arnhold, A. Pichert, The influence of glycosaminoglycans on IL-8-mediated functions of neutrophils, Carbohydr. Res. 356 (2012) 196–203.
[36] B. Meyer, T. Peters, NMR Spectroscopy techniques for screening and identifying ligand binding to protein receptors, Angew. Chem. Int. Ed. 42 (2003) 864–890.
[37] Y. Shen, F. Delaglio, G. Cornilescu, A. Bax, TALOS+: a hybrid method for predicting protein backbone torsion angles from NMR chemical shifts, J. Biomol. NMR 44 (2009) 213–223.
[38] S. Theisgen, H.A. Scheidt, A. Magalhaes, T.J. Bonagamba, D. Huster, A solid-state NMR study of the structure and dynamics of the myristoylated N-terminus of the guanylate cyclase-activating protein-2, Biochim. Biophys. Acta 1798 (2010) 266–274.
[39] T. Schröder, H. Lilie, C. Lange, The myristoylation of guanylate cyclase-activating protein-2 causes an increase in thermodynamic stability in the presence but not in the absence of Ca^{2+}, Protein Sci. 20 (2011) 1155–1165.
[40] S. Bagby, K.I. Tong, M. Ikura, Optimization of protein solubility and stability for protein nuclear magnetic resonance, Methods Enzymol. 339 (20–41) (2001) 20–41.
[41] J. Anglister, S. Grzesiek, H. Ren, C.B. Klee, A. Bax, Isotope-edited multidimensional NMR of calcineurin B in the presence of the non-deuterated detergent CHAPS, J. Biomol. NMR 3 (1993) 121–126.
[42] J.B. Ames, T. Porumb, T. Tanaka, M. Ikura, L. Stryer, Amino-terminal myristoylation induces cooperative calcium binding to recoverin, J. Biol. Chem. 270 (1995) 4526–4533.
[43] C.R. Sanders, F. Sonnichsen, Solution NMR of membrane proteins: practice and challenges, Magn. Reson. Chem. 44 (2006) S24–S40 (Spec No).
[44] W.D. Van Horn, H.J. Kim, C.D. Ellis, A. Hadziselimovic, E.S. Sulistijo, M.D. Karra, C.L. Tian, F.D. Sonnichsen, C.R. Sanders, Solution Nuclear Magnetic Resonance Structure of Membrane-Integral Diacylglycerol Kinase, Science 324 (2009) 1726–1729.
[45] A. Vogel, G. Reuther, K. Weise, G. Triola, J. Nikolaus, K.T. Tan, C. Nowak, A. Herrmann, H. Waldmann, R. Winter, D. Huster, The lipid modifications of Ras that sense membrane environments and induce local enrichment, Angew. Chem. Int. Ed. 48 (2009) 8784–8787.
[46] L.P. Haynes, R.D. Burgoyne, Unexpected tails of a Ca^{2+} sensor, Nat. Chem. Biol. 4 (2008) 90–91.
[47] J.N. Wingard, J. Ladner, M. Vanarotti, A.J. Fisher, H. Robinson, K.T. Buchanan, D.M. Engman, J.B. Ames, Structural insights into membrane targeting by the flagellar calcium-binding protein (FCaBP), a myristoylated and palmitoylated calcium sensor in Trypanosoma cruzi, J. Biol. Chem. 283 (2008) 23388–23396.
[48] H. Kollmann, S.F. Becker, J. Shirdel, A. Scholten, A. Ostendorp, C. Lienau, K.W. Koch, Probing the Ca^{2+} switch of the neuronal Ca^{2+} sensor GCAP2 by time-resolved fluorescence spectroscopy, ACS Chem. Biol. 7 (2012) 1006–1014.
[49] S. Hovmoller, T. Zhou, T. Ohlson, Conformations of amino acids in proteins, Acta Crystallogr. D Biol. Crystallogr. 58 (2002) 768–776.
[50] Y. Shen, A. Bax, SPARTA+: a modest improvement in empirical NMR chemical shift prediction by means of an artificial neural network, J. Biomol. NMR 48 (2010) 13–22.